# Analysis of the angular acceptance of surface plasmon Bragg mirrors

María Ujué González,[1,2,*] Andrey L. Stepanov,[3,4] Jean-Claude Weeber,[2] Andreas Hohenau,[3] Alain Dereux,[2] Romain Quidant,[1,5] and Joachim R. Krenn[3]

[1]*ICFO–Institut de Ciencies Fotoniques, Mediterranean Technology Park, 08860 Castelldefels (Barcelona), Spain*
[2]*Laboratoire de Physique de l'Université de Bourgogne, UMR CNRS 5027, 9 Avenue A. Savary, BP 47870, F-21078 Dijon, France*
[3]*Institute of Physics, Karl-Franzens-University, Universitätsplatz 5, 8010 Graz, Austria*
[4]*Kazan Physical-Technical Institute RAN, Sibirsky Trakt 10/7, 420029 Kazan, Russian Federation*
[5]*ICREA–Institució Catalana de Recerca i Estudis Avançats, 08010 Barcelona, Spain*
[*]*Corresponding author: Maria-Ujue.Gonzalez@icfo.es*

Received June 20, 2007; revised August 5, 2007; accepted August 11, 2007;
posted August 14, 2007 (Doc. ID 84220); published September 6, 2007

We analyze an important aspect of the behavior of surface plasmon polariton (SPP) Bragg mirrors: the dependence of the angular acceptance for reflection on the incidence angle. By means of leakage radiation microscopy, both in direct and Fourier space, we observe that the angular acceptance diminishes for increasing incidence angles. This effect, which can considerably affect the design of devices based on these elements, is shown to be the consequence of the decrease of the bandgap width with increasing incidence angle. © 2007 Optical Society of America

*OCIS codes:* 240.6680, 230.3120, 230.1480, 260.3910, 130.3120.

Surface plasmon based photonics is already recognized as a promising route for obtaining miniaturized optical devices [1]. The realization of future plasmonic chips requires the development of elements capable of controlling the propagation of surface plasmon polaritons (SPPs). So far, several key functionalities have already been demonstrated [2–4]. Among the proposed SPP elements, SPP Bragg mirrors have received particular attention [4,5]. Actually, Bragg mirrors are considered not only relevant elements on their own, but also integrated in other elements [6,7] or as building blocks for more complex devices, such as beam splitters [8], interferometers [4], or SPP launchers [9].

Different configurations have been proposed to act as SPP Bragg mirrors, and their reflectance properties have been analyzed [5]. There are, however, aspects of the performance of these devices not yet considered, which could have important consequences for their implementation. In this work we study the angular acceptance for reflection of SPP Bragg mirrors as a function of the angle of incidence, $\alpha_{inc}$. This property, defined as the range of angles of incidence that are reflected by a Bragg mirror designed for a given $\alpha_{inc}$ and wavelength, can be crucial when Bragg mirrors are to be integrated in waveguides, or used to filter different propagation directions.

The analyzed samples, fabricated by electron beam lithography, consist of gratings of 10 Au lines, 60 nm high and 150 nm wide, lying on a 70 nm thick Au layer. This kind of Bragg mirror has been proved to be very efficient, with reflectance values close to 100% [5]. The periodicity of the grating, $d$, for the system to act as an SPP Bragg mirror for a SPP wavelength, $\lambda_{SPP}$ and $\alpha_{inc}$, is

$$d = \frac{\lambda_{SPP}}{2\cos\alpha_{inc}}. \quad (1)$$

Figure 1(a) shows the scanning electron microscope (SEM) image of one of the fabricated samples for $\alpha_{inc}=30°$. The sample is composed of a Bragg mirror and a diffracting line placed 30 $\mu$m away from the mirror. This diffracting line is used to locally launch two counterpropagating SPPs by focusing on it a perpendicularly incident laser beam (free-space wavelength $\lambda_0=800$ nm), as sketched in Fig. 1(a). The angular spreading of the SPPs excited in this way is controlled by the numerical aperture of the focusing objective. Figure 1(a) also includes the definition of $\alpha_{inc}$ and the propagation direction of the most relevant SPP wave vectors, $k_{SP}$.

The interaction of the Bragg mirrors with SPPs propagating on the metal film has been characterized by means of leakage radiation (LR) microscopy, a far-field technique that provides images whose intensity is proportional to that of the propagating SPP [10]. Figure 1(b) shows the evolution of the angular acceptance for reflection of SPP Bragg mirrors as a function of the incidence angle for four values of $\alpha_{inc}$: 0°, 30°, 45°, and 60°. For each mirror, the periodicity has been adjusted for the desired $\alpha_{inc}$ according to Eq. (1). In the absence of the mirror (SPP freely propagating toward the right), we have found that the divergence of the incident plasmon is 32° by plotting the intensity distribution of the SPP beam along a line parallel to the diffracting line [see dashed line in Fig. 1(c)]. In spite of this wide angular divergence, the SPP beam traveling toward the left-hand side is fully reflected (no transmission is detected after the mirror) for $\alpha_{inc}=0°$. As the angle of incidence increases, the most divergent in-plane k-vectors of the beam are not reflected any more, and in transmission two lateral beams appear. The width of this lateral beam increases with $\alpha_{inc}$, while the portion of the reflected beam gets narrower. Profiles across the transmitted beams give the angular aperture for which no trans-

0146-9592/07/182704-3/$15.00 

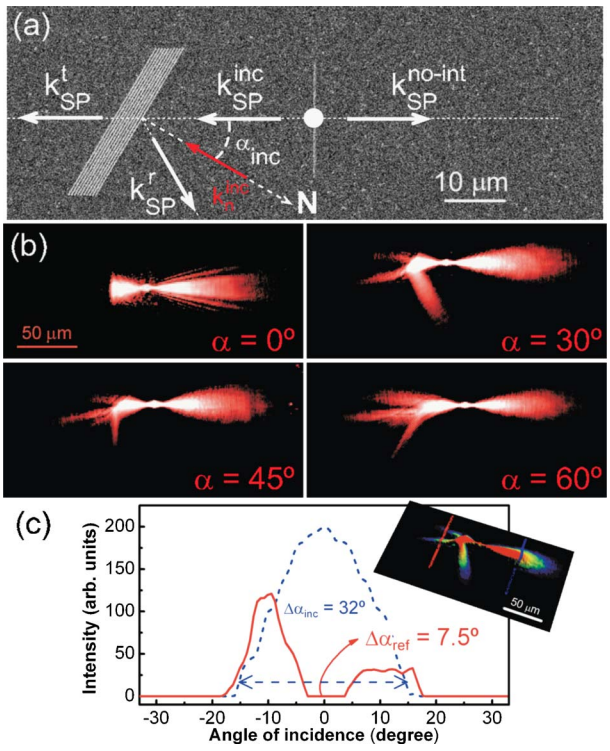


Fig. 1. (Color online) (a) SEM image of one fabricated SPP Bragg mirror ($\alpha_{inc}=30°$ here). The wave vectors ($k_{SP}$) of the incident (inc), reflected (r), transmitted (t) and free propagating (no-int) surface plasmons are sketched in the figure. (b) Leakage radiation images of SPPs impinging on mirrors at $\alpha_{inc}=0°$, 30°, 45°, and 60°. (c) Intensity cross-cuts along the lines as indicated in the inset (Bragg mirror at 30°). The dashed (blue) line shows the angular spreading of the incident beam; the solid (red) line corresponds to the transmitted beam.

**Table 1. Evolution with $\alpha_{inc}$ of the Acceptance Angle for Reflection, $\Delta\alpha_{ref}$ (°), for SPP Bragg Mirrors[a]**

| | LR, exp. | | Theo. | |
|---|---|---|---|---|
| $\alpha_{inc}$ (°) | Mirrors | Fourier | Disp. | Isofreq. |
| 0 | >32 | 49±1.0 | 59.5 | 58 |
| 30 | 7.5±0.5 | 6±1.0 | 10.5 | 10 |
| 45 | 3.5±0.5 | 3.5±1.0 | 3.9 | 4.8 |
| 60 | 2±0.5 | 1.4±0.5 | 0.6 | 1.7 |

[a]LR columns correspond to the experimental values extracted from LR images of Bragg mirrors (mirrors) and the Fourier plane of gratings (Fourier). Theo. columns summarize the values extracted from the calculated dispersion (Disp.) and isofrequency (Isofreq.) diagrams.

mission is detected, which we identify as the angular acceptance for reflection, $\Delta\alpha_{ref}$. For instance, for $\alpha_{inc}=30°$ this angular acceptance is 7.5°. The values obtained in this way for different angles of incidence are summarized in Table 1. The results show that the SPP Bragg mirror's angular acceptance for reflection strongly decreases as $\alpha_{inc}$ increases.

The reflectivity of the considered kind of SPP mirrors is based on the 1D photonic bandgap opened by a Bragg grating. The analysis of the dispersion relation of SPPs propagating on corrugated surfaces can thus help us to understand this angular dependence. To obtain these dispersion relations we have computed, by using the differential method [11,12], the reflectivity under *p*-polarized incidence of a 70 nm thick gold film on glass whose upper interface is textured by a grating of gold ridges (60 nm high, 150 nm wide) with rectangular profiles, analogous to the Au lines used to fabricate our SPP Bragg mirrors. The minima in the reflectivity of this corrugated thin film are associated to the excitation of surface modes, thus providing the dispersion relation of SPP propagating on it.

Figure 2(a) shows the dispersion diagram obtained for a surface decorated with a grating of periodicity $d=455$ nm when the SPP travels at 30° from the grating normal ($\alpha_{inc}=30°$). As expected from Eq. (1), a bandgap around $\lambda_0=800$ nm appears at the edge of the first Brillouin zone. Figure 2(b) summarizes the evolution of the bandgap width for different $\alpha_{inc}$, all of them for systems intended for having gaps at $\lambda_0=800$ nm. It can be observed that, as $\alpha_{inc}$ increases, the bandgap width decreases, in good agreement with the behavior observed for $\Delta\alpha_{ref}$ as well as with the result shown in Ref. [13]. A coarse calculation can be used to translate the bandgap width to $\Delta\alpha_{ref}$. In reciprocal space Eq. (1) can be written as $\mathbf{G}=2\mathbf{k}_n^{inc}$, with $\mathbf{G}$ the reciprocal vector of the Bragg grating, and $\mathbf{k}_n^{inc}$ the projection of the incident SPP wave vector along the grating normal [$\mathbf{k}_n^{ing}=(2\pi/\lambda_{SSP})\cos\alpha_{inc}$]. A finite width bandgap implies that a range of $\mathbf{k}_n^{inc}$, can indeed be reflected. For fixed $\alpha_{inc}$ this corresponds to the energy gap $\Delta\lambda_{SPP}$ given by the dispersion diagram. If we now fix $\lambda_{SPP}$ we can calculate the $\alpha_{inc}$ gap, that is, $\Delta\alpha_{ref}$. The $\Delta\alpha_{ref}$ values obtained from this calculation are included in Table 1, showing good agreement with the experimental results coming from the LR images of the mirrors.

To get a deeper insight of the SPP on the analyzed gratings, we consider the isofrequency contour diagrams of the system. These diagrams provide the behavior of a SPP propagating along all the different directions of the surface. They can also be calculated as the dispersion diagrams above, i.e., by obtaining the reflectivity maps of the films for a fixed energy and *p*-polarized light incident in all directions. Moreover, the isofrequency contours can be experimentally obtained by means of leakage radiation measurements [14]. In fact, an appropriate lens set in the LR micro-

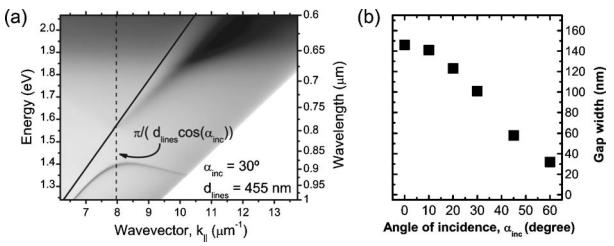


Fig. 2. (a) Calculated dispersion relation for SPP propagating on a Au surface decorated with a Bragg grating. The solid line represents the light line. The dashed line delimits the first Brillouin zone. (b) Evolution of the bandgap width with $\alpha_{inc}$.

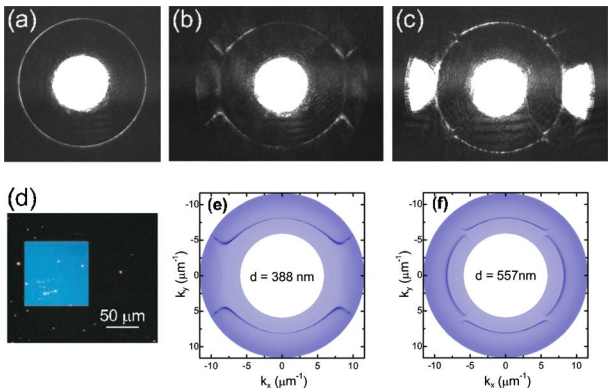


Fig. 3. (Color online) Experimental LR images, obtained at $\lambda_0 = 800$ nm, of the Fourier plane of SPP propagating on (a) homogeneous Au film, 60 nm thick; (b) Au film decorated with a grating ($d = 388$ nm) of Au lines, 60 nm high; (c) film with a grating of $d = 557$ nm. (d) Dark-field image of one grating. (e), (f) Calculated isofrequency ($\lambda_0 = 800$ nm) contour maps for a SPP propagating on a grating of $d = 388$ nm and $d = 557$ nm.

scope allows to image either the sample or the Fourier plane [10].

Figures 3(a)–3(c) show the obtained LR images, at $\lambda_0 = 800$ nm, of the Fourier plane of SPP propagating on a flat Au surface, on a grating with $d = 388$ nm, and on a grating with $d = 557$ nm. To obtain these images, 100 $\mu$m $\times$ 100 $\mu$m gratings of Au lines have been fabricated on top of a Au film [see Fig. 3(d)]. The SPP is then coupled through the intrinsic defects present on the Au film and gratings by focusing an unpolarized laser beam at its surface (the central bright spot in the Fourier plane is due to the excitation beam). For a homogeneous Au film the SPP can propagate in all directions, hence a whole circle can be seen in Fig. 3(a). For the gratings, SPP modes with wave vector $\mathbf{k} \pm \mathbf{G}$ can also be excited due to the interaction with the grating. Therefore, in the Fourier plane we will observe three circles corresponding to the SPP Bloch modes in the first and second Brillouin zones [14]. Where two circles interact [also given by Eq. (1)], the bandgap opens and SPP propagation is prevented in that direction [Figs. 3(b) and 3(c)]. From these images, the angular extension of the gap can be determined, and the obtained results are shown in Table 1. The agreement with the angular acceptance values for reflectance obtained for the Bragg mirrors is very good. Finally, Figs. 3(e) and 3(f) show the calculated isofrequency diagrams for $d = 388$ nm and $d = 557$ nm at $\lambda_0 = 800$ nm, which are in excellent accord with the experimental images. The theoretical $\Delta\alpha_{ref}$ obtained in a direct way from these calculations are also included in Table 1.

We have investigated the dependence of the angular acceptance for reflection on the angle of incidence in SPP Bragg mirrors. The acceptance range decreases for increasing $\alpha_{inc}$, and is in fact quite broad for small angles of incidence. We have demonstrated the relation between this effect and the bandgap width of the dispersion relation of SPP propagating on equivalent corrugated surfaces. These effects have important consequences for the design of devices based on Bragg mirrors, if high angular or spectral selectivity is required. Moreover, it also opens perspectives for the design of new structures based on these properties, such as the already demonstrated one-dimensional plasmonic crystal [15].

This work was supported by the European Network of Excellence Plasmo-Nano-Devices. M.U.G. thanks the Spanish Ministry of Education for funding under the "Ramón y Cajal" program. A.L.S. is grateful to the Lisa Meitner programme of the Austrian Scientific Foundation and the Russian Foundation for Basic Research, grant 06-02-08147, for their support.

## References

1. E. Ozbay, Science **311**, 189 (2006).
2. S. I. Bozhevolnyi, V. S. Volkov, E. Devaux, J. Y. Laluet, and T. W. Ebbesen, Nature **440**, 508 (2006).
3. J. A. Dionne, H. J. Lezec, and H. A. Atwater, Nano. Lett. **6**, 1928 (2006).
4. H. Ditlbacher, J. R. Krenn, G. Schider, A. Leitner, and F. R. Aussenegg, Appl. Phys. Lett. **81**, 1762 (2002).
5. M. U. González, J.-C. Weeber, A.-L. Baudrion, A. Dereux, A. L. Stepanov, J. R. Krenn, E. Devaux, and T. W. Ebbesen, Phys. Rev. B **73**, 155416 (2006).
6. V. S. Volkov, S. I. Bozhevolnyi, E. Devaux, J.-Y. Laluet, and T. W. Ebbesen, Nano. Lett. **7**, 880 (2007).
7. S. Jetté-Charbonneau, R. Charbonneau, N. Lahoud, G. Mattiussi, and P. Berini, Opt. Express **13**, 4674 (2005).
8. J.-C. Weeber, M. U. González, A.-L. Baudrion, and A. Dereux, Appl. Phys. Lett. **87**, 221101 (2005).
9. F. López-Tejeira, S. G. Rodrigo, L. Martín-Moreno, F. J. García-Vidal, E. Devaux, T. W. Ebbesen, J. R. Krenn, I. P. Radko, S. I. Bozhevolnyi, M. U. González, J. C. Weeber, and A. Dereux, Nat. Phys. **3**, 324 (2007).
10. A. Drezet, A. Hohenau, A. L. Stepanov, H. Ditlbacher, B. Steinberger, N. Galler, F. R. Aussenegg, A. Leitner, and J. R. Krenn, Appl. Phys. Lett. **89**, 091117 (2006).
11. M. Nevière and E. Popov, *Light Propagation in Periodic Media: Differential Theory and Design* (Basel, 2003).
12. L. Li, J. Opt. Soc. Am. A **13**, 1024 (1996).
13. A. Yu. Nikitin and L. Martín-Moreno, Phys. Rev. B **75**, 081405(R) (2007).
14. A. Giannattasio and W. L. Barnes, Opt. Express **13**, 428 (2005).
15. J.-C. Weeber, A.-L. Baudrion, A. Bouhelier, A. Bruyant, G. C. des Francs, R. Zia, and A. Dereux, Appl. Phys. Lett. **89**, 211109 (2006).